The Journal of Infectious Diseases

MAJOR ARTICLE

Evolution of Spatial Risk of Malaria Infection After a Pragmatic Chemoprevention Program in Response to Severe Flooding in Rural Western Uganda

Erin Xu,[1,a] Varun Goel,[2,3,a] Emmanuel Baguma,[4] Emmanuel Ayebare,[4] Brandon D. Hollingsworth,[5] Amanda Brown-Marusiak,[6] Dana Giandomenico,[7] Raquel Reyes,[6] Moses Ntaro,[4] Edgar M. Mulogo,[4] and Ross M. Boyce[3,7,8]

[1]School of Medicine, UNC School of Medicine; [2]Department of Geography; [3]Carolina Population Center, University of North Carolina at Chapel Hill; [4]Department of Community Health, Faculty of Medicine, Mbarara University of Science and Technology, Uganda; [5]Department of Entomology, Cornell University, Ithaca, New York; [6]Division of Hospital Medicine; [7]Department of Epidemiology, Gillings School of Global Public Health; and [8]Institute for Global Health and Infectious Diseases, University of North Carolina at Chapel Hill

Background. Malaria epidemics result from extreme precipitation and flooding, which are increasing with global climate change. Local adaptation and mitigation strategies will be essential to prevent excess morbidity and mortality.

Methods. We investigated the spatial risk of malaria infection at multiple timepoints after severe flooding in rural western Uganda employing longitudinal household surveys measuring parasite prevalence and leveraging remotely sensed information to inform spatial models of malaria risk in the 3 months after flooding.

Results. We identified clusters of malaria risk emerging in areas (1) that showed the greatest changes in Normalized Difference Vegetation Index from pre- to postflood and (2) where residents were displaced for longer periods of time and had lower access to long-lasting insecticidal nets, both of which were associated with a positive malaria rapid diagnostic test result. The disproportionate risk persisted despite a concurrent chemoprevention program that achieved high coverage.

Conclusions. The findings enhance our understanding not only of the spatial evolution of malaria risk after flooding, but also in the context of an effective intervention. The results provide a "proof of concept" for programs aiming to prevent malaria outbreaks after flooding using a combination of interventions. Further study of mitigation strategies—and particularly studies of implementation—is urgently needed.

Keywords. climate change; flooding; malaria; *Plasmodium*.

Climate change will impact the burden of many vector-borne diseases, including malaria, posing new challenges to control programs [1–3]. In addition to rising surface temperatures, climate change increases both the frequency and intensity of severe weather events such as droughts and floods [4–6]. An estimated 1.8 billion people, representing approximately 23% of the world population, are directly exposed to 1-in-100-year floods, including 176 million in sub-Saharan Africa [7]. Nearly half of the global disasters over the past 2 decades were attributable to extreme precipitation and flooding [8]. While not all flood events are a direct consequence of anthropogenic climate change, any increase in frequency or severity is likely to have a substantial public health impact. Local adaptation and mitigation strategies are essential to preventing excess morbidity and mortality in the near term.

Unlike the immediate health impacts of flooding (eg, displacement, drowning), malaria tends to emerge in later phases of recovery [9, 10]. Heavy precipitation is thought to flush established larval habitats, an effect that can result in short-term reductions in transmission [11, 12]. As floodwaters recede, however, malaria vectors establish new breeding sites in the many pools of standing water, resulting in a surge in disease weeks to months after the event [13–15]. Despite the established relationship between flooding and malaria—with >60 relevant publications identified in 1 review of the topic—there are significant issues in study designs, including lack of comparator groups (eg, data from the preflood period or from unaffected areas), the absence of individual- or household-level data, and limited follow-up [10, 16–18]. These issues may be partly due to the unpredictability of such events, as well as the challenging conditions encountered in a disaster context, which can make access to affected areas difficult.

On 5 May 2020, local rivers in Kasese district began to overflow their banks causing displacement of >100 000 residents (Figure 1) [19, 20]. The flooding was preceded by a 30-day period of daily rainfall (Supplementary Figure 1). While extreme, this highland region experiences frequent episodes of heavy

Received 29 December 2022; editorial decision 08 August 2023; accepted 14 August 2023; published online 16 August 2023

[a]E. X. and V. G. contributed equally to this work.

Presented in part: Annual Meeting of the American Society of Tropical Medicine and Hygiene, Seattle, Washington, 30 October–3 November 2022.

Correspondence: Ross M. Boyce, MD, MSc, Division of Infectious Diseases, University of North Carolina at Chapel Hill, 111 Mason Farm Road, Chapel Hill, NC 27514, USA (roboyce@med.unc.edu).

The Journal of Infectious Diseases® 2024;229:173–82

© The Author(s) 2023. Published by Oxford University Press on behalf of Infectious Diseases Society of America. All rights reserved. For permissions, please e-mail: journals.permissions@oup.com

https://doi.org/10.1093/infdis/jiad348



Figure 1. Aftermath of severe flooding in Bugoye subcounty following heavy rainfall in May 2020. Image courtesy of Emmanuel Baguma.

rainfall almost every May, the end of the traditional rainy season. Over the past decade, these periods of severe rainfall have resulted in more frequent flooding events. Anthropogenic drivers of this increase include climate change and land use changes [21]. Our previous work after a similar flood event in 2013 demonstrated a 30% increase in the relative risk (RR) of testing positive for malaria in the 12-month postflood period as compared to the preflood period [22]. However, this study was ecological in design, utilizing villages as the unit of analysis, and therefore did not explore potential associations between malaria incidence and individual households or more fine-scale geographic characteristics.

In response to the most recent event, we performed a prospective analysis of the spatial factors influencing household malaria risk at multiple time points after flooding in 1 impacted village. To achieve this goal, we relied heavily on geographical information systems (GISs), which previous studies have shown can improve the understanding of the spatial and temporal distribution of vector-borne diseases [23, 24]. Specifically, we hypothesized that GISs could be employed longitudinally in a disaster setting to not only identify "hotspots" of disease but also to facilitate the selective targeting of interventions and assess potential gaps in program implementation amid a rapidly evolving environment [25–29].

METHODS

Study Site

Izinga village is located in the Maliba subcounty of Kasese District (0.3006 N, 30.1059 E). The village lies within a valley at the foothills of the Rwenzori Mountains and is bordered by the Mubuku River to the west and the Kitajuka River to the east with the 2 rivers intersecting in both the north and south (Figure 2*A*). The village occupies an area of approximately 1.3 km^2 with a population of 1118 residents living in 188 distinct households. More than one-third (38.1%) of residents are children <12 years of age [18]. The climate in the Kasese District is characterized by a biannual wet season that sustains year-round malaria transmission with seasonal peaks in January and July. *Anopheles gambiae* and *Anopheles funestus* are thought to be the primary malaria vectors in the region [30–32]. *Plasmodium falciparum* accounts for the vast majority (>95%) of malaria infections [33, 34], with reported *P falciparum* parasitemia rates ranging between 7.3% and 17.4% in the wider region according to the most recent malaria indicator surveys [21, 22].

Study Design

In response to severe flooding in May 2020, we carried out a pragmatic chemoprevention intervention to mitigate a postflood surge in malaria. In brief, children ≤12 years of age were eligible to receive 3 monthly rounds of dihydroartemisinin-piperaquine (DP) beginning approximately 30 days after the flood (Figure 3). The methods and results of the program have been previously reported [35]. Below, we report the methods relevant to this analysis.

Preflood Survey

In March 2020, we carried out a cross-sectional survey of 60 households in Izinga village as part of an ongoing project [36]. In brief, after consent was obtained, study staff recorded the household location using a handheld global positioning system (GPS) and administered a brief questionnaire that elicited responses about care-seeking behaviors, long-lasting insecticidal net (LLIN) sourcing and use, and recent health status. Axillary temperature was measured and 50 µL of capillary blood drawn for a malaria rapid diagnostic test (RDT) (SD

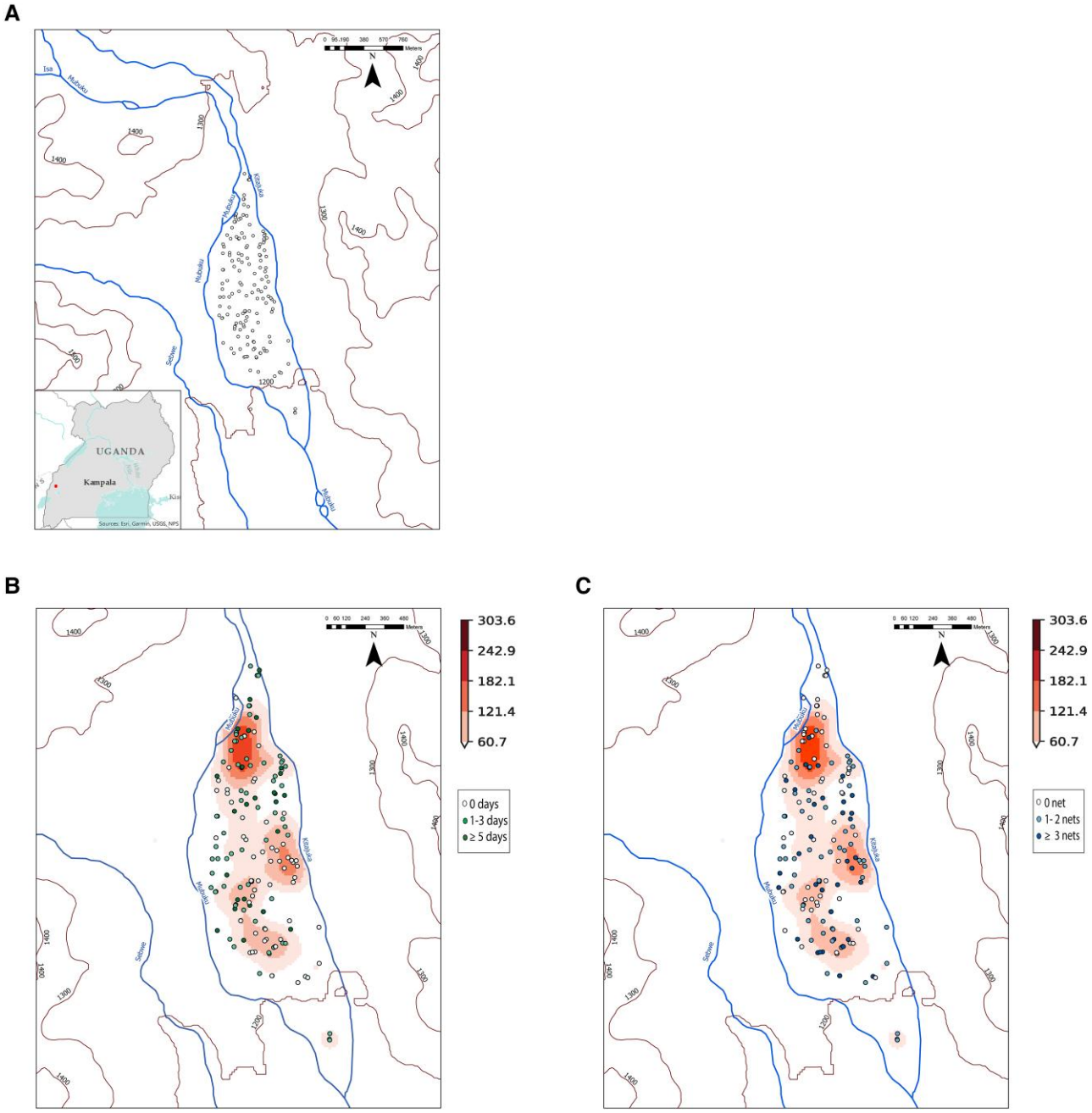


Figure 2. *A,* Map of Izinga village with location of participating households (circles) and key terrain features. *B* and *C,* Kernel density analysis of malaria rapid diagnostic test results presented as cases per square kilometer approximately 1 month after flooding, with shaded areas indicating areas of high prevalence of *Plasmodium falciparum* parasitemia overlaid on days of displacement due to flooding (*B*) and long-lasting insecticidal net ownership (*C*) as assessed 1 month postflooding.

Bioline Malaria Ag P.f., Abbott Laboratories). RDT results were recorded as either positive or negative, with faint lines being considered positive.

Postflood Surveys

The first survey in the postflood period was launched on 10 June 2020, approximately 1 month after the flood. Local community health workers guided field staff to all households in their respective area of responsibility. When a household eligible for the chemoprevention intervention (ie, at least 1 child aged ≤12 years in the home) was reached, the adult caregiver was asked to provide verbal consent for participation. Staff recorded the household location using a handheld GPS device, then administered a brief questionnaire that elicited responses about displacement due to the flooding, incident malaria cases since the flood, and LLIN ownership and use (Supplementary

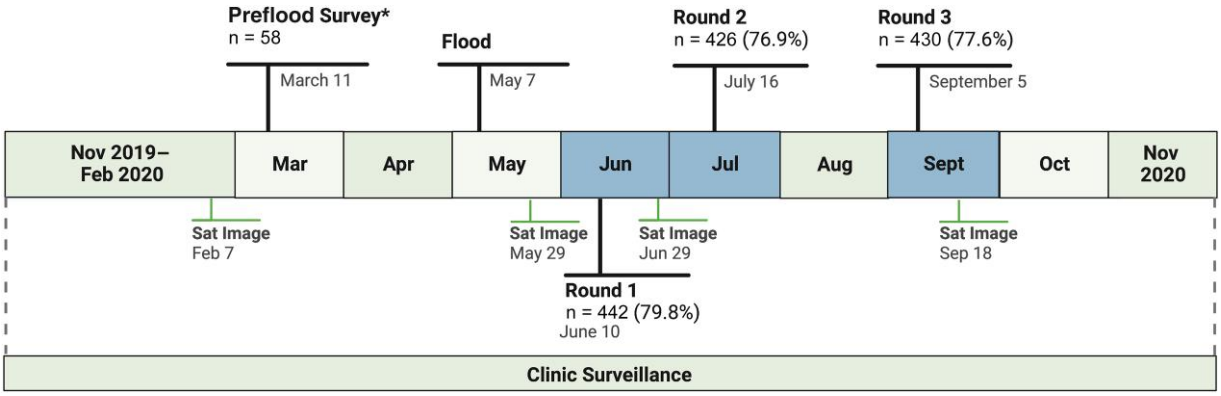


Figure 3. Timeline of events including flooding, each round of chemoprevention including number of children receiving chemoprevention and estimated proportion of coverage, and period of clinic surveillance. Figure previously published in related article (Boyce et al. [35]). Figure created with BioRender.com. *Preflood survey was conducted in Izinga village as part of unrelated, ongoing study of malaria transmission in the area. Abbreviation: Sat, satellite.

Material). Before administering the first dose of DP, 50 µL of capillary blood was drawn for a malaria RDT, the results of which were recorded on the case report form. Similar surveys were repeated in July and September 2020 (Figure 3).

Data Management and Statistical Analysis

Data Management

All information was recorded in and uploaded to a secure electronic database (REDCap) using smartphones [37]. After each survey, data were cleaned by manual review, including correction of minor typographical errors in latitude and longitude. Households were defined as all individuals who report residing at a particular set of latitude and longitude coordinates or having the same caregiver. In the case where individuals reported the same latitude and longitude but different caregivers, we confirmed that both caregivers were known to live together. Individuals without a reported latitude and longitude were grouped by caregiver, and each individual caregiver was assumed to be a separate household.

Statistical and Spatial Analysis

The primary outcome of interest was *P falciparum* parasite prevalence, defined as the number of individuals with a positive RDT result per round. Our explanatory variables included calendar time, which we divided into "preflood" and 3 "postflood" periods, and the location of each household. We described the demographic characteristics, LLIN access and usage, and the extent of displacement experienced by households across the flooding periods. We also calculated the Normalized Difference Vegetation Index (NDVI), a measure of vegetation greenness, to examine the vegetation density in the study area during time periods before and after the flood. To calculate the NDVI, we acquired publicly available imageries from the Landsat 8 program at a spatial resolution of 30 m, and a temporal resolution of 16 days from both the pre- and postflood (1-, 2- and 3-month) periods. To remove the effects of cloud cover and terrain occlusion, we also utilized the quality assessment band provided for each image to mask any areas that were not considered "clear terrain." We conducted similar analyses with other variables including the Normalized Difference Water Index, Modified Normalized Difference Water Index, and the Soil-Adjusted Vegetation Index to assess the extent of the flooding (Supplementary Figures 2, 3 and Tables 1, 2).

To visualize geographic variation in malaria transmission from pre- to postflooding, we estimated kernel-smoothed spatial relative risk surfaces across the study area for each survey round [38, 39]. The spatial relative risk estimator, constructed as a ratio of the kernel density of cases (RDT-positive locations) to the kernel density of controls (RDT-negative locations), describes the risk of malaria at a particular location compared to the expected malaria risk in the same location [40, 41]. We calculated a relative risk surface of malaria prevalence using an adaptive symmetric kernel smoothing bandwidth [42].

Last, to identify clusters of malaria prevalence, we applied a Kulldorff spatial scan statistic using a purely spatial Bernoulli model to identify areas where the observed incidence of disease within a cluster window is significantly higher compared to the expected incidence across the entire study area [43]. We ran the model using a maximum cluster size of 50% of the total population and used 99 999 Monte Carlo simulations to generate *P* values. We then superimposed clusters of significantly higher malaria RR ($P < .05$) on the relative risk surfaces for each survey round. This enabled us to visualize areas where malaria risk increased (values >1) or decreased (values <1) postflooding compared to the baseline preflood malaria risk. All kernel-smoothed relative risk surfaces were edge corrected and created using the R package sparr version 2.2-15 [44], while Kulldorff spatial scan statistics and clusters were generated using SaTScan version 9.7 [43].

Ethical Approvals

Ethical approval was provided by the institutional review boards of the University of North Carolina at Chapel Hill (19-1094), the Mbarara University of Science and Technology (06/05-18), and the Uganda National Council for Science and Technology (HS 2482).

RESULTS

Preflood

The preflood survey was conducted on 11 March 2020. Satellite imagery from February demonstrates high NDVI across the vast majority of the village (Figure 4*A*). Lower NDVI values are observed following the path of the Mubuku River along the western border of the village, whereas the Kitajuka River to the east is more difficult to distinguish. Lower NDVI values in this area could be seen, suggesting reduced water levels and/or the presence of healthy vegetation. During the survey, a total of 18 of the 60 children tested had a positive malaria RDT result, representing a weighted estimate of 30.0% (95% confidence interval, 24.8%–35.8%) *P falciparum* parasitemia rate prior to flooding [36]. As shown in Figure 5*A*, spatial analysis demonstrated increased risk of malaria in the northernmost areas, particularly those to the northeast along the border with the Mubuku River, and much of the southern half of the village. Both of these are relatively lush, flat areas, although not obviously different from other parts of the village. The scan statistic, however, did not identify any significant clusters of infection.

Postflood

One Month Postflooding

Satellite imagery obtained in late May (Figure 4*B*), approximately 1 week after the flood but before the first postflood survey, showed visibly lower NDVI values in the northern areas of the village near the divergence of the Mubuku and Kitajuka rivers. Such changes in the NDVI could be attributable to (1) loss of healthy vegetation caused by violent floodwaters and/or (2) the presence of increased surface water. Additionally, the course of the rivers is much more clearly defined, which could be a result of substantially higher water levels.

The first postflood survey was conducted 10–13 June 2020, approximately 1 month after the flood. Study staff visited 158 households, reaching 442 children 12 years of age and younger, assumed to represent approximately 80% of the eligible population. Displacement as a result of flooding was widely reported, but the respondents living in the northern areas of the village—generally the same areas with the greatest reductions in NDVI—reported the highest rates and longest periods of displacement (Figure 2*B*). Similarly, reported access to LLINs was lowest here (Figure 2*C*), although overall ownership and reported use was well below World Health Organization targets, which may be partly due to the flood event occurring toward the end of a 3-year distribution cycle [45].

A total of 102 (23.1%) children tested prior to DP administration had a positive RDT result. At least 1 child with a positive RDT result was present in 67 (42.4%) households, while multiple children were positive in 25 (15.8%) households. Characteristics of children are summarized in Table 1. Notably, children with a positive RDT result were less likely

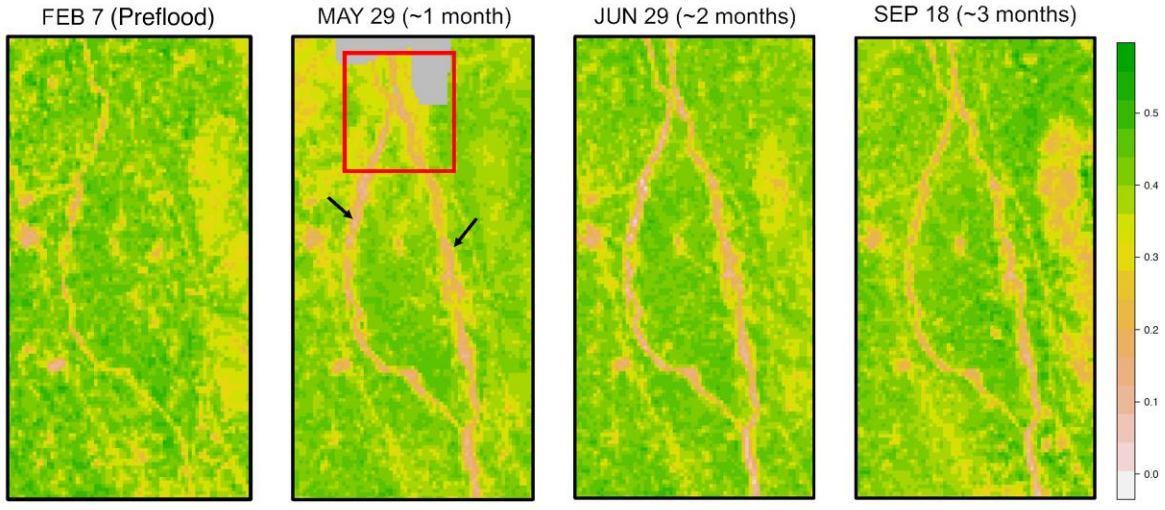


Figure 4. Normalized Difference Vegetation Index (NDVI) over the study period. Higher values signify areas with greater vegetation density, whereas lower values represent areas with minimal to no healthy vegetation such as water (eg, rivers) or more urban settlements. Notably, imagery obtained after flooding (7 May 2020) shows substantial decreases in NVDI in areas along the banks of the Mubuku and Kitajuka rivers (arrows) as well as the northern areas of Izinga village where the rivers diverge (box).

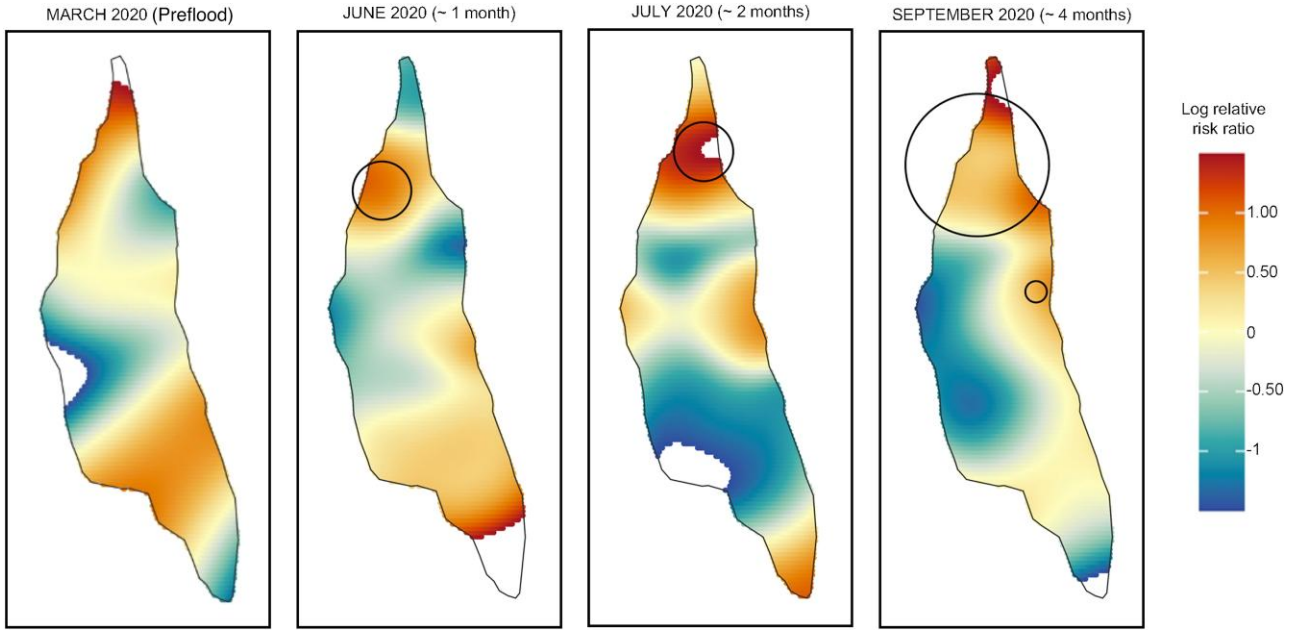


Figure 5. Spatial relative risk of malaria for each time period using an adaptive kernel density and results of SaTScan scanning statistic. The kernel density surface estimates the relative risk of malaria at each location compared to the expected malaria risk at that location for the given time period. The circles indicate clusters of statistically significantly higher malaria risk than expected, based on results from SaTScan, which begin to emerge in northern areas of the village 1–2 months after flooding, consistent with reestablishment of breeding sites in flood-impacted areas.

Table 1. Characteristics of Households Surveyed Approximately 1 Month Postflooding, Stratified by Malaria Rapid Diagnostic Test Result

Characteristic	RDT Negative	RDT Positive[a]	*P* Value[b]
Demographic characteristics			
Households, No. (%)	56 (35.4)	102 (64.6)	
No. of children in household, median (IQR)	3.0 (1.0–4.0)	3.0 (2.0–5.0)	**<.01**
Age of children, y, median (IQR)	7.0 (5.0–9.0)	6 (5.0–8.0)	.08
LLIN availability and use			
Any LLIN in the household, No. (%)	34 (69.3)	53 (55.7)	.12
No. of LLIN in household, median (IQR)	2.0 (0.0–3.0)	1.0 (0.0–5.0)	**<.01**
Proportion of children sleeping under LLIN, mean (range)	26.7 (0.0–100.0)	0.0 (0.0–50.0)	.06
Displacement			
Household displaced by flooding, No. (%)	32.0 (65.3)	90.0 (62.5)	1.0
Days displaced by flooding, median (IQR)	3.0 (1.0–4.0)	3 (1.0–5.0)	.28
Malaria episodes			
No. of children RDT positive, median (IQR)	0.0 (0.0–0.0)	1.0 (1.0–3.0)	
No. of children with reported malaria cases, median (IQR)	0.0 (0.0–1.0)	1 (0.0–1.8)	**.02**
No. of children treated for malaria, median (IQR)	0.0 (0.0–1.0)	1.0 (0.0–1.0)	**.04**

Values in bold represents $P < .05$.

Abbreviations: IQR, interquartile range; LLIN, long-lasting insecticidal net; RDT, rapid diagnostic test.

[a]At least 1 positive RDT within the household.

[b]*P* values determined using Mann–Whitney and Pearson χ^2 tests for means/medians and proportions, respectively.

to have slept under an LLIN the previous night (52.6% vs 68.8%; $P = .02$) and more likely to report a malaria case in the interval period since the flood (49.0% vs 19.4%; $P < .001$).

When compared to the baseline survey, the spatial distribution of malaria risk in the village after the flood appears to have shifted to areas that were previously less at risk, although a foci of transmission intensity indicated by a SaTScan cluster (RR, 2.41; $P = .030$) remained in the northwest portion of the village (Figure 5*B*).

Two Months Postflooding

Satellite imagery obtained in late June (Figure 4*C*), approximately 2 months after the flood, continued to demonstrate low NDVI values along the course of the rivers, but values in the northernmost areas of the village had returned to baseline levels, which may indicate the natural resolution of surface water.

The second survey was then conducted 16–24 July 2020. Study staff reached 426 children, 381 (89.4%) of whom had participated in the first round. A total 62 (14.6%) children had a positive malaria RDT result. Approximately one-third (20 [37.7%]) of children with a positive result were positive during the first round, while 19 (31.2%) reported an episode of symptomatic malaria requiring health seeking in the interval period. There were 10 (16.1%) children who had a positive RDT in both rounds and also reported at least 1 malaria episode between rounds. Notably, among these 10 children were 3 pairs of

siblings, all of whom had been displaced to a temporary encampment immediately after the flooding. Furthermore, only 3 of these 10 children were reported to have slept under an LLIN the previous night.

Spatially, the risk of malaria was lower across most of the village after the first round of chemoprevention, although risk remained highest in the north with a continued hotspot (RR, 7.61; $P = .037$) near the divergence of the 2 rivers (Figure 5*C*).

Three Months Postflooding

The third and final survey was conducted 5–8 September 2020. Satellite imagery from this time (Figure 4*D*) demonstrates that the NDVI is largely unchanged from the prior month. A total of 428 children, representing >75% of the eligible population, were reached. A total of 80 (18.7%) children had a positive malaria RDT result. Again, a relatively high proportion of those children who had tested positive in the second round were positive again (17/53 [32.1%]) or reported an incident malaria episode (18/80 [22.5%]).

Spatially, while the RR of malaria incidence decreased in the southern part of the study area as compared to the baseline, the risk was higher in north and northeastern Izinga. While the northern area continued to be a hotspot (RR, 5.57; $P = .023$), a second likely hotspot also emerged in the northeast (RR, 2.46; $P = .079$).

Overall, a majority of eligible children (n = 335 [60.5%]) participated in all 3 surveys, while an additional 78 (14.1%) participated in 2 rounds. In a sensitivity analysis examining the number of chemoprevention doses administered, we did not observe any spatial differences (ie, clustering) of low uptake, defined as <3 doses received. LLIN ownership and usage, along with displacement attributable to flooding, were not significantly different between participants in each round. Households where at least 1 RDT was positive over the study period tended to have more children ($P = .007$) and fewer LLINs in the household ($P < .001$) than households without a positive RDT result.

DISCUSSION

Our study, unique for the fact that it was conducted in the context of a natural disaster and chemoprevention intervention, highlights the rapid evolution of environmental conditions and malaria risk following severe precipitation and flooding. Yet even with the chemoprevention program, which our prior analysis shows to have had a significant impact on malaria transmission [35], there remained considerable spatial variability in malaria risk across different timepoints after flooding. Specifically, we observed the emergence of malaria hotspots in northern areas of the village that had (1) greater rates of reported displacement and (2) greater changes in NDVI values, both of which suggest that these areas were disproportionately impacted by flooding. Overall, these findings serve as a valuable "proof of concept" as to how GIS tools when combined with rapid household surveys can be utilized to guide ongoing humanitarian response, highlighting areas that may require additional interventions to control malaria outbreaks as conditions evolve.

Consistent with previous studies, we observed that parasite prevalence was not substantially higher in the northernmost areas of the village in the period immediately after flooding. This effect may have resulted from the "flushing" of larval habitats in the areas that were most severely flooded [37]. However, these areas also experienced a relatively rapid and intense rebound in parasite prevalence. In contrast, less severely affected areas to the south, where brick making [46, 47] and other human activities may normally sustain transmission, did not experience a comparable rebound. One hypothesis to explain this difference is that the northern areas of the village were inherently more suitable environments for mosquito breeding, and the abundance of standing water in the postflood period accelerated reestablishment of larval habitats. Furthermore, the northern areas of the village are more densely populated, which may have contributed to importation of parasites from surrounding villages as residents returned home or traveled to market areas. While preliminary, these findings are consistent with prior studies showing that chemoprevention may have a greater relative and more durable impact in areas where transmission is already less intense [48, 49]. In higher-transmission settings, complementary measures such as indoor residual spraying or larval source management may be needed to control postflood malaria outbreaks.

We also observed that households in the northern areas experienced longer periods of displacement, which was associated with positive RDT results. Most displaced residents reported staying with family members in less affected villages or in temporary camps set up by relief organizations, locations which may not have been amenable to LLIN use. While it is not possible to completely disentangle the complex factors driving individual malaria risk, the likelihood that displacement contributed to lower LLIN use is noteworthy. Humanitarian response programs should not only ensure that temporary housing solutions can accommodate LLINs, but also develop contingencies for rapid distributions to bring affected households back up to universal coverage targets [45]. Interventions such as insecticide-treated blankets that do not require hanging may also be effective in this setting [50]. Last, our work highlights that in areas repeatedly impacted by severe flooding, longer-term interventions such as improved floodwater control (eg, riverbank stabilization, retaining walls) and policy solutions such as incentivizing residents to relocate permanently from vulnerable areas may be required.

Our study has a number of strengths including the serendipitous collection of data in the months immediately prior to

flooding, the repeated measurements in the 3 months after flooding, and the high rate of community participation. At the same time, our analysis also has a number of important limitations. Foremost of these is the relatively small geographic area of the study, which reduced the availability of cloud-free satellite imagery around critical time periods. Additionally, due to a relatively small sample size, our cluster analysis does not account for covariates that may explain some of the elevated malaria risk clusters in the study area. For example, what covariates we did collect were at the household rather than individual level—a decision made to facilitate more efficient delivery of the intervention amid a disaster setting, but one that also limits our ability to perform more complex analyses. Last, the ongoing chemoprevention program likely disrupted transmission, thereby limiting our ability to observe the natural evolution of malaria risk. Unequal uptake of the chemoprevention intervention, particularly if there were spatial differences, could have confounded our analysis. We are, however reassured by the relatively high and consistent coverage rates achieved as demonstrated by the absence of spatial clustering observed in our sensitivity analysis.

CONCLUSIONS

We observed a dynamic evolution of spatial malaria risk after severe flooding in a rural highland area of western Uganda. Notably, this disparate spatial risk emerged even amid an ongoing chemoprevention intervention that achieved high coverage among the target population. Compared to the preflood period, malaria risk increased disproportionately in the areas that appeared most affected by flooding. Overall, our findings provide a proof of concept for the application of GIS tools to guide malaria control efforts in response to severe flooding. Further studies over larger areas are needed to operationalize potential interventions and refine criteria for use.

Supplementary Data

Supplementary materials are available at *The Journal of Infectious Diseases* online. Consisting of data provided by the authors to benefit the reader, the posted materials are not copyedited and are the sole responsibility of the authors, so questions or comments should be addressed to the corresponding author.

Notes

Author contributions. Study conception and design: R. M. B., E. X., R. R., E. B., E. M. M. Funding: R. M. B. Study implementation: R. M. B., E. X., E. B., M. N., E. M. M. Data analysis: E. X., B. D. H., V. G., R. M. B. First draft of manuscript: E. X., V. G., R. M. B. Revisions: All authors.

Acknowledgments. We wish to thank the residents of Izinga village who participated in the study. In addition, we recognize the support of the Kasese District Health Office, which facilitated study implementation.

Data availability. Deidentified individual data that support the results will be shared beginning 9–36 months following publication, provided that the investigator who proposes to use the data has approval from an institutional review board, independent ethics committee, or research ethics board, as applicable, and executes a data use/sharing agreement with the University of North Carolina.

Financial support. R. M. B. is supported by the National Institutes of Health (award number K23AI141764) and received additional funds from a Caregivers at Carolina Award made by the Doris Duke Charitable Foundation (award number 2015213). V. G. acknowledges support from the Eunice Kennedy Shriver National Institute of Child Health and Human Development (award number P2C HD050924). E. X. acknowledges the support of a Benjamin H. Kean Travel Fellowship from the American Society of Tropical Medicine and Hygiene. Database support was provided by the North Carolina Translational and Clinical Sciences Institute, which is supported by the National Center for Advancing Translational Sciences, National Institutes of Health (grant number UL1TR002489).

Potential conflicts of interest. All authors: No reported conflicts.

All authors have submitted the ICMJE Form for Disclosure of Potential Conflicts of Interest. Conflicts that the editors consider relevant to the content of the manuscript have been disclosed.

References

1. Mora C, McKenzie T, Gaw IM, et al. Over half of known human pathogenic diseases can be aggravated by climate change. Nat Clim Chang **2022**; 12:869–75.
2. Caminade C, McIntyre KM, Jones AE. Impact of recent and future climate change on vector-borne diseases. Ann N Y Acad Sci **2019**; 1436:157–73.
3. Rocklöv J, Dubrow R. Climate change: an enduring challenge for vector-borne disease prevention and control. Nat Immunol **2020**; 21:479–83.
4. Hirabayashi Y, Mahendran R, Koirala S, et al. Global flood risk under climate change. Nat Clim Chang **2013**; 3: 816–21.
5. Dankers R, Arnell NW, Clark DB, et al. First look at changes in flood hazard in the Inter-Sectoral Impact Model Intercomparison Project ensemble. Proc Natl Acad Sci U S A **2014**; 111:3257–61.
6. Mora C, Spirandelli D, Franklin EC, et al. Broad threat to humanity from cumulative climate hazards intensified by greenhouse gas emissions. Nat Clim Chang **2018**; 8: 1062–71.
7. Rentschler J, Salhab M, Jafino BA. Flood exposure and poverty in 188 countries. Nat Commun **2022**; 13:3527.

8. . Centre for Research on the Epidemiology of Disasters/United Nations Office for Disaster Risk Reduction (UNDRR). Human cost of disasters: an overview of the last 20 years (2000–2019). . Geneva, Switzerland: UNDRR, **2020**.
9. Du W, FitzGerald GJ, Clark M, Hou XY. Health impacts of floods. Prehosp Disaster Med **2010**; 25:265–72.
10. Charnley GEC, Kelman I, Gaythorpe KAM, Murray KA. Traits and risk factors of post-disaster infectious disease outbreaks: a systematic review. Sci Rep **2021**; 11:5616.
11. Lindsay SW, Bodker R, Malima R, Msangeni HA, Kisinza W. Effect of 1997–98 El Niño on highland malaria in Tanzania. Lancet **2000**; 355:989–90.
12. Paaijmans KP, Wandago MO, Githeko AK, Takken W. Unexpected high losses of *Anopheles gambiae* larvae due to rainfall. PLoS One **2007**; 2:e1146.
13. Brown V, Abdir Issak M, Rossi M, Barboza P, Paugam A. Epidemic of malaria in north-eastern Kenya. Lancet **1998**; 352:1356–7.
14. Kondo H, Seo N, Yasuda T, et al. Post-flood–infectious diseases in Mozambique. Prehosp Disaster Med **2002**; 17:126–33.
15. Elsanousi YEA, Elmahi AS, Pereira I, Debacker M. Impact of the 2013 floods on the incidence of malaria in Almanagil locality, Gezira state, Sudan. PLoS Curr **2018**:10. doi:10.1371/currents.dis.8267b8917b47bc12ff3a712fe4589fe1.
16. Okaka FO, Odhiambo BDO. Relationship between flooding and out break of infectious diseases in Kenya: a review of the literature. J Environ Public Health **2018**; 2018:1–8.
17. Suhr F, Steinert JI. Epidemiology of floods in sub-Saharan Africa: a systematic review of health outcomes. BMC Public Health **2022**; 22:268.
18. Coalson JE, Anderson EJ, Santos EM, et al. The complex epidemiological relationship between flooding events and human outbreaks of mosquito-borne diseases: a scoping review. Environ Health Perspect **2021**; 129:96002.
19. FloodList. Uganda—thousands affected by floods in Western Region. http://floodlist.com/africa/uganda-thousands-affected-by-floods-in-western-region. Accessed 23 March 2021.
20. Okiror S. "People are desperate": floods and rock slides devastate western Uganda. London: The Guardian; **2023**.
21. Taylor RG, Mileham L, Tindimugaya C, Mwebembezi L. Recent glacial recession and its impact on alpine riverflow in the Rwenzori Mountains of Uganda. J Afr Earth Sci **2009**; 55:205–13.
22. Boyce R, Reyes R, Matte M, et al. Severe flooding and malaria transmission in the western Ugandan highlands: implications for disease control in an era of global climate change. J Infect Dis **2016**; 214:1403–10.
23. Zhao X, Thanapongtharm W, Lawawirojwong S, et al. Malaria risk map using spatial multi-criteria decision analysis along Yunnan border during the pre-elimination period. Am J Trop Med Hyg **2020**; 103:793–809.
24. Kelly GC, Hale E, Donald W, et al. A high-resolution geospatial surveillance-response system for malaria elimination in Solomon Islands and Vanuatu. Malar J **2013**; 12:108.
25. Clements AC, Reid HL, Kelly GC, Hay SI. Further shrinking the malaria map: how can geospatial science help to achieve malaria elimination? Lancet Infect Dis **2013**; 13:709–18.
26. Gebreslasie MT. A review of spatial technologies with applications for malaria transmission modelling and control in Africa. Geospat Health **2015**; 10:328.
27. Hamre KES, Hodges JS, Ayodo G, John CC. Lack of consistent malaria incidence hotspots in a highland Kenyan area during a 10-year period of very low and unstable transmission. Am J Trop Med Hyg **2020**; 103:2198–207.
28. Huang JX, Xia ZG, Zhou SS, et al. Spatio-temporal analysis of malaria vectors in national malaria surveillance sites in China. Parasit Vectors **2015**; 8:146.
29. Leonard CM, Assefa A, Sime H, et al. Spatial distribution of *Plasmodium falciparum* and *Plasmodium vivax* in northern Ethiopia by microscopic, rapid diagnostic test, laboratory antibody, and antigen data. J Infect Dis **2022**; 225:881–90.
30. Lynd A, Gonahasa S, Staedke SG, et al. LLIN evaluation in Uganda Project (LLINEUP): a cross-sectional survey of species diversity and insecticide resistance in 48 districts of Uganda. Parasit Vectors **2019**; 12:94.
31. Mawejje HD, Kilama M, Kigozi SP, et al. Impact of seasonality and malaria control interventions on *Anopheles* density and species composition from three areas of Uganda with differing malaria endemicity. Malar J **2021**; 20:138.
32. Ojuka P, Boum Y III, Denoeud-Ndam L, et al. Early biting and insecticide resistance in the malaria vector *Anopheles* might compromise the effectiveness of vector control intervention in southwestern Uganda. Malar J **2015**; 14:148.
33. Yeka A, Gasasira A, Mpimbaza A, et al. Malaria in Uganda: challenges to control on the long road to elimination: I. Epidemiology and current control efforts. Acta Trop **2012**; 121:184–95.
34. Boyce R, Reyes R, Matte M, Ntaro M, Mulogo E, Siedner MJ. Use of a dual-antigen rapid diagnostic test to screen children for severe *Plasmodium falciparum* malaria in a high-transmission, resource-limited setting. Clin Infect Dis **2017**; 65:1509–15.
35. Boyce RM, Hollingsworth BD, Baguma E, et al. Dihydroartemisinin-piperaquine chemoprevention and malaria incidence after severe flooding: evaluation of a pragmatic intervention in rural Uganda. Clin Infect Dis **2021**;73:e3124–6.
36. Cote CM, Goel V, Muhindo R, et al. Malaria prevalence and long-lasting insecticidal net use in rural western

Uganda: results of a cross-sectional survey conducted in an area of highly variable malaria transmission intensity. Malar J **2021**; 20:304.
37. Harris PA, Taylor R, Thielke R, Payne J, Gonzalez N, Conde JG. Research electronic data capture (REDCap)—a metadata-driven methodology and workflow process for providing translational research informatics support. J Biomed Inform **2009**; 42:377–81.
38. Wheeler DC. A comparison of spatial clustering and cluster detection techniques for childhood leukemia incidence in Ohio, 1996–2003. Int J Health Geog **2007**; 6:13.
39. Sarojinie Fernando WTP, Hazelton ML. Generalizing the spatial relative risk function. Spat Spatiotemporal Epidemiol **2014**; 8:1–10.
40. Bithell JF. An application of density estimation to geographical epidemiology. Stat Med **1990**; 9:691–701.
41. Kelsall JE, Diggle PJ. Kernel estimation of relative risk. Bernoulli **1995**; 1:3–16.
42. Davies TM, Hazelton ML. Adaptive kernel estimation of spatial relative risk. Stat Med **2010**; 29:2423–37.
43. Kulldorff M. A spatial scan statistic. Commun Stat Theory Methods **1997**; 26:1481–96.
44. R Core Team. R: A language and environment for statistical computing. https://www.R-project.org/. Accessed 22 November 2022.
45. World Health Organization (WHO). Achieving and maintaining universal coverage with long-lasting insecticidal nets for malaria control. Geneva, Switzerland: WHO; **2017**.
46. Carlson JC, Byrd BD, Omlin FX. Field assessments in western Kenya link malaria vectors to environmentally disturbed habitats during the dry season. BMC Public Health **2004**; 4:33.
47. Paul P, Kangalawe RYM, Mboera LEG. Land-use patterns and their implication on malaria transmission in Kilosa District, Tanzania. Trop Dis Travel Med Vaccines **2018**; 4:6.
48. Mwesigwa J, Achan J, Affara M, et al. Mass drug administration with dihydroartemisinin-piperaquine and malaria transmission dynamics in The Gambia: a prospective cohort study. Clin Infect Dis **2019**; 69:278–86.
49. Eisele TP, Bennett A, Silumbe K, et al. Short-term impact of mass drug administration with dihydroartemisinin plus piperaquine on malaria in Southern Province, Zambia: a cluster-randomized controlled trial. J Infect Dis **2016**; 214:1831–9.
50. Azizi S, Matowo J, Mbewe NJ, et al. Laboratory and semi-field efficacy evaluation of permethrin–piperonyl butoxide treated blankets against pyrethroid-resistant malaria vectors. Sci Rep **2022**; 12:22166.